# Structural Studies of the Molybdenum Site in the MoFe Protein and Its FeMo Cofactor by EXAFS

**Steven D. Conradson,[1a] Barbara K. Burgess,[1b] William E. Newton,[1c] Leonard E. Mortenson,[1d] and Keith O. Hodgson*[1e]**

*Contribution from the Department of Chemistry, Stanford University, Stanford, California 94305, Western Regional Research Center, USDA—ARS, Albany, California 94710, Department of Molecular Biology and Biochemistry, University of California at Irvine, Irvine, California 92717, and Department of Biological Sciences, Purdue University, West Lafayette, Indiana 47907.* *Received March 7, 1986*

**Abstract:** Nitrogenase is a complex bacterial enzyme system that is responsible for the conversion of atmospheric $N_2$ to ammonia. The structure and function of molybdenum in the MoFe protein of this system has been the subject of a number of investigations, including the use of X-ray absorption spectroscopy. This paper reports the results of our recent studies on several states of the MoFe protein and its FeMo cofactor (which is extruded by treatment with *N*-methylformamide). Mo K-edge (XANES) and extended fine structure (EXAFS) spectra have been recorded to high energies above the absorption edge with excellent signal-to-noise on the semireduced form of the MoFe protein from both *Clostridium pasteurianum* and *Azotobacter vinelandii* and on the as isolated FeMo-co and FeMo-co treated with benzenethiol and with benzeneselenol. In all of the states studied, EXAFS results reveal that the Mo is in an environment that contains two or three oxygen (or nitrogen) atoms at 2.10–2.12 Å, three to five S atoms at 2.37 Å, and three to four Fe atoms at 2.68–2.70 Å. The numbers of these ligands change upon removal of the cofactor from the protein as discussed in the paper. For FeMo-co, comparisons also show that thiol/selenol is not binding directly to the Mo site. The results of these EXAFS (and our XANES published earlier) definitely show the presence of several low-*Z* ligands and are not compatible with a tetrahedral arrangement of only nearest S neighbors at the Mo site.

Nitrogenase is the complex, bacterial enzyme system that catalyzes the biological conversion of atmospheric dinitrogen to ammonia. The complexity of the system is clearly illustrated by both its genetic organization[2] and by its numerous requirements for turnover.[3] The enzyme system consists of two separately purifiable proteins, MgATP, a low-potential reductant, the ubiquitous protons, and an anaerobic environment. The putative reductant in vivo is either a ferredoxin or flavodoxin, while dithionite is the reductant of choice in vitro. A number of other small molecules, such as $C_2H_2$, HCN, RNC, $N_3^-$, $HN_3$, and $N_2O$, are alternative substrates that can be reduced by nitrogenase.

The smaller of the two component proteins, the Fe protein, acts as an ATP-binding, specific electron donor to the larger MoFe protein. The MoFe protein incorporates at least six metal-containing prosthetic groups,[4-7] two of which constitute the iron–molybdenum cofactors (FeMo-co). Only limited information has accrued concerning either the structure or the functional role in the catalytic process of these prosthetic groups. However, recent genetic evidence strongly implicates FeMo-co as the site of $N_2$ binding and reduction.[8] Since its first extrusion from the protein matrix,[9] FeMo-co has elicited much interest both in its own right as an apparently unique heterometallic cluster of composition $MoFe_{6-8}S_{4-9}$[9-12] and as a simplified vehicle with which to probe the Mo environment of nitrogenase.[12-15] The elucidation of the structure[16,17] of FeMo-co and the determination of its catalytic properties[16c,18,19] are recognized as significant challenges that, when solved, will set major goals for the bioinorganic chemist.[20]

The unique Mo atom in each FeMo-co presents a logical target for investigation. However, although FeMo-co is the source of the biologically unique $S = {}^3/_2$ spin system of the MoFe protein of nitrogenase, which produces its distinctive EPR signal,[21] the

(1) (a) Stanford University. Present address: Los Alamos National Laboratory, Los Alamos, NM 87545. (b) University of California at Irvine. (c) Western Regional Research Center, USDA, and Department of Biochemistry and Biophysics, University of California at Davis. Former address: Charles F. Kettering Research Laboratory, Yellow Springs, OH 45387. (d) Purdue University. Present address: Department of Biochemistry, University of Georgia, Athens, GA 30602. (e) Stanford University.

(2) Kennedy, C.; Cannon, F.; Cannon, M.; Dixon, R.; Hill, S.; Jensen, J.; Kumar, S.; McLean, P.; Merrick, M.; Robson, R.; Postgate, J. *Current Perspectives in Nitrogen Fixation*; Gibson, A. H., Newton, W. E., Eds.; Elsevier/North Holland: New York, 1981; p 146. Roberts, G. P.; Brill, W. J. *Annu. Rev. Microbiol.* **1981**, *35*, 207.

(3) (a) Thorneley, R. N. F.; Mortenson, L. E. *Annu. Rev. Biochem.* **1979**, *48*, 387. (b) Burgess, B. K. In *Advances in Nitrogen Fixation Research*; Veeger, C., Newton, W. E., Eds.; Martinus Nijhoff: The Hague, 1984; p 103.

(4) Kurtz, D. M., Jr.; McMillan, R. S.; Burgess, B.K.; Mortenson, L. E.; Holm, R. H. *Proc. Natl. Acad. Sci. U.S.A.* **1979**, *76*, 4986.

(5) (a) Munck, E.; Rhodes, H.; Orme-Johnson, W. H.; Davis, L. C.; Brill, W. J.; Shah, V. K. *Biochim. Biophys. Acta* **1975**, *400*, 32. (b) Zimmermann, R.; Munck, E.; Brill, W. J.; Shah, V. K.; Henzl, M. T.; Rawlings, J.; Orme-Johnson, W. H. *Biochim. Biophys. Acta* **1978**, *537*, 185. (c) Hunyh, B. H.; Munck, E.; Orme-Johnson, W. H. *Biochim. Biophys. Acta* **1979**, *576*, 192.

(6) Smith, J. P.; Emptage, M. H.; Orme-Johnson, W. H. *J. Biol. Chem.* **1982**, *257*, 2310.

(7) (a) Watt, G. D.; Burns, A.; Lough, S.; Tennent, D. L. *Biochemistry* **1980**, *19*, 4926. (b) Watt, G. D.; Burns, A.; Tennent, D. L. *Biochemistry* **1981**, *20*, 7272. (c) Lough, S.; Burns, A.; Watt, G. D. *Biochemistry* **1983** *22*, 4062.

(8) Hawkes, T. R.; McLean, P. A.; Smith, B. E. *Biochem. J.* **1984**, *217*, 317.

(9) Shah, V. K.; Brill, W. J. *Proc. Natl. Acad. Sci. U.S.A.* **1977**, *74*, 3249.

(10) Yang, S.-S.; Pan, W.-H.; Friesen, G. D.; Burgess, B. K.; Corbin, J. L.; Stiefel, E. I.; Newton, W. E. *J. Biol. Chem.* **1982**, *257*, 8042.

(11) Nelson, M. J.; Levy, M. A.; Orme-Johnson, W. H. *Proc. Natl. Acad. Sci. U.S.A.* **1983**, *80*, 147.

(12) Burgess, B. K.; Newton, W. E. In *Nitrogen Fixation: The Chemical–Biochemical–Genetic Interface*; Müller, A., Newton, W. E., Eds.; Plenum: New York, 1983; p 83.

(13) Robinson, A. E.; Richards, A. J. M.; Thomson, A. J.; Hawkes, T. R.; Smith, B. E. *Biochem. J.* **1984**, *219*, 495.

(14) (a) Hoffman, B. M.; Roberts, J. E.; Orme-Johnson, W. H. *J. Am. Chem. Soc.* **1982**, *104*, 860. (b) Hoffman, B. M.; Venters, R. A.; Nelson, M. J.; Orme-Johnson, W. H. *J. Am. Chem. Soc.* **1982**, *104*, 4711.

(15) Shah, V. K.; Ugalde, R. A.; Imperial, J.; Brill, W. J. *J. Biol. Chem.* **1985**, *260*, 3891.

(16) (a) Cramer, S. P.; Hodgson, K. O.; Gillum, W. O.; Mortenson, L. E. *J. Am. Chem. Soc.* **1978**, *100*, 3398. (b) Cramer, S. P.; Gillum, W. O.; Hodgson, K. O.; Mortenson, L. E.; Stiefel, E. I.; Chisnell, J. R.; Brill, W. J.; Shah, V. K. *J. Am. Chem. Soc.* **1978**, *100*, 3814. (c) Newton, W. E.; Burgess, B. K.; Cummings, S. C.; Lough, S.; McDonald, J. W.; Rubinson, J. F.; Conradson, S. D.; Hodgson, K. O. In *Advances in Nitrogen Fixation Research*; Veeger, C., Newton, W. E., Eds.; Martinus Nijhoff: The Hague, 1984; p 160. (d) Wolff, T. F.; Berg, J. M.; Warrick, C.; Hodgson, K. O.; Holm, R. H.; Frankel, R. B. *J. Am. Chem. Soc.* **1978**, *100*, 4630.

(17) Antonio, M. R.; Teo, B.-K.; Orme-Johnson, W. H.; Nelson, M. J.; Groh, S. E.; Lindahl, P. A.; Kauzlarich, S. M.; Averill, B. A. *J. Am. Chem. Soc.* **1982**, *104*, 4703.

(18) Rawlings, J.; Shah, V. K.; Chisnell, J. R.; Brill, W. J.; Zimmerman, R.; Munck, E.; Orme-Johnson, W. H. *J. Biol. Chem.* **1978**, *253*, 1001.

(19) (a) Burgess, B. K.; Stiefel, E. I.; Newton, W. E. *J. Biol. Chem.* **1980**, *255*, 353. (b) Schultz, F. A.; Gheller, S. F.; Burgess, B. K.; Lough, S.; Newton, W. E. *J. Am. Chem. Soc.* **1985**, *107*, 5364.

(20) (a) Holm, R. H. *Chem. Soc. Rev.* **1981**, *10*, 455. (b) Coucouvanis, D. *Acc. Chem. Res.* **1981**, *14*, 201. (c) Averill, B. A. *Struct. Bonding (Berlin)* **1983**, *53*, 59.

0002-7863/87/1509-7507$01.50/0 

**Table I.** Sample Characteristics

| sample no. | sample type (organism) | [Mo], mM | Fe/Mo | additions | activity[a] before | activity[a] after | exptl session |
|---|---|---|---|---|---|---|---|
| 1 | semireduced MoFe protein (*Cp*) | 1.62 | 14.5 | | 1810 | 1650 | A |
| 2 | semireduced MoFe protein (*Cp*) | 1.51 | 15.1 | | 1980 | 1870 | A |
| 3 | semireduced MoFe protein (*Av*) | 0.70 | 15.6 | | 2150 | 1974 | B |
| 4 | FeMo-co (cit/phos) | 0.56 | 6.85 | | 276 | 263 | C |
| 5 | FeMo-co (cit/phos) | 1.33 | 7.10 | | 224 | 194 | D |
| 6 | FeMo-co (HCl/NaOH) | 0.62 | 7.02 | | 256 | 232 | A |
| 7 | FeMo-co (HCl/NaOH) | 0.61 | 7.02 | PhSH | 256 | 229 | A |
| 8 | FeMo-co (cit/phos) | 1.32 | 7.10 | PhSH | 224 | 224 | D |
| 9 | FeMo-co (HCl/NaOH) | 0.61 | 7.02 | PhSeH | 256 | 231 | A |

[a] For semireduced MoFe protein samples, activity data are expressed as nanomoles of $H_2$/minute per milligram of protein; for FeMo-co samples, as nanomoles of $C_2H_4$/minute per nanomole of MO after *Av* UW45 reconstitution.

Mo atoms appear to play only a rather limited role in the EPR properties. Similarly, the applications of many other spectroscopic techniques to this problem[13,14] have met with only limited success. A single, notable exception is X-ray absorption spectroscopy (XAS).[21,22]

Analysis of the XAS can provide structural and electronic information about a given absorbing element.[22] Thus, XAS has been a very useful probe of the Mo environment of FeMo-co both in and after extrusion from the MoFe protein matrix.[16,23] Our studies have utilized the two independent, but complementary, aspects of XAS. The so-called XANES,[21,22] which includes the X-ray absorption edge and near-edge regions, provides details of the electronic structure, first coordination sphere, and site symmetry of the absorbing atom. The EXAFS region,[21,22] which begins above the absorption edge, provides metrical details, as well as the numbers and types of atoms surrounding the absorber.

Our original Mo EXAFS analyses of the MoFe protein provided the first indications of the cluster nature of the Mo-containing complex in FeMo-co. These studies demonstrated Fe and S atoms to be the nearest-neighbor atoms to Mo, with sulfur being at a sulfide-like bridge-bonding distance.[16] Subsequent iron EXAFS studies of FeMo-co are in accord with such a structure.[17] Our recently reported nitrogenase Mo XANES spectra[23] are also consistent with this cluster structure for FeMo-co. However, these XANES analyses, which include both FeMo-co samples bound within the protein and as the free entity (in both isolated and chemically modified forms), have given added structural insights. The XANES spectra of all MoFe protein and FeMo-co samples were found to closely resemble those of synthetic clusters containing a $MoS_3O_3$ coordination sphere.

Since the initial EXAFS reports, a variety of inorganic Mo–Fe–S–O clusters have been synthesized,[20] for which we have now analyzed the EXAFS spectra. This study significantly increases our database for evaluating the reliability of EXAFS structural determinations on Mo-containing enzymes. In addition, detection systems for recording XAS data and the quality and quantity of radiation available from synchrotron sources used for these experiments have markedly improved since the earlier measurements. Consequently, we have been able to collect EXAFS data of significantly enhanced quality. The data have been collected to achieve a wider range of data in $k$ space and better signal-to-noise on several previously studied protein samples as well as new chemically modified samples of FeMo-co. The samples investigated include the dithionite-reduced state of both the MoFe protein (referred to as "semireduced") and extruded FeMo-co plus FeMo-co treated with an excess of either benzenethiol or benzeneselenol.

## Experimental Section

**1. MoFe Protein Samples. (a) *Clostridium pasteurianum* Samples.** The MoFe protein of *C. pasteurianum* (*Cp*) was prepared by modifications of a previous method.[24] It was purified by starting with extracts made from thawed, frozen cells and using, in series, gradient elutions from columns of DE-52 (Whatman), DEAE Sepharose CL-6B, and DEAE Sephacel (Pharmacia). Acetylene reduction assays were performed as described in ref 25. The purified MoFe protein had a specific activity of 1600–1800 nmol of $C_2H_2$ formed $min^{-1}$ per mg of protein and showed only the two MoFe protein subunits when examined by gel electrophoresis. The Mo and Fe contents were 1.8 and 29 ± 1 mol/mol of MoFe protein tetramer, respectively. For EXAFS experiments, solutions were concentrated to 180–190 mg of protein/mL (1.56 ± 0.06 mM in Mo).

**(b) *Azotobacter vinelandii* Samples.** The MoFe protein was purified to homogeneity as previously described,[26] except that, at the last step, the crystalline sample (ca. 300 mg) was dissolved in 2.5 mL of 0.025 M Tris-HCl, pH 7.4, which was 0.35 M in NaCl and 1.2 mM in $Na_2S_2O_4$. The resulting semireduced protein sample was 0.70 mM in Mo and had a specific activity of 2150 before and 1974 nmol $H_2$ $min^{-1}$ per mg of protein after the experimental run (Table I). Mo (1.9 mol/mol) and Fe (30 mol/mol) were analyzed by standard techniques.[27,28] Protein samples were frozen initially in liquid $N_2$ and transported to the Stanford Synchrotron Radiation Laboratory (SSRL) in serum vials stored in dry ice.

**2. Iron–Molybdenum Cofactor Samples.** For all FeMo-co preparations, highly purified MoFe protein from *A. vinelandii* (*Av*)[26] was used. As indicated in Table I, two different methods were employed for FeMo-co preparation. The citric acid/phosphate method was performed by a modification[10] of the original isolation method.[9] The large-scale HCl/NaOH isolation was performed as previously described.[10] All samples were concentrated by the vacuum distillation technique[26] and centrifuged to remove precipitated salts and denatured protein. When PhSH or PhSeH was added, anaerobic solutions were prepared in *N*-methylformamide (NMF) by the freeze–pump–thaw method at concentrations that would give a 10-fold excess of reagent over Mo when 0.1 mL was added to 1 mL of FeMo-co solution. The samples were stored anaerobically and frozen in dry ice in serum vials for transport to SSRL.

The analyses for Fe[27] and Mo[28] in Table I represent means of triplicate determinations with standard deviations of less than 8%. The *Av* UW45 reconstitution activity assays[9] used extracts of cells grown and prepared as described previously.[26] These concentrated FeMo-co samples were diluted 1:10 with NMF (which was 1.2 mM in $Na_2S_2O_4$ before addition to the *Av* UW45 extracts). Reconstitution was effected by a 30-min incubation of a 1–4-μL aliquot of diluted FeMo-co with 0.3 mL of *Av* UW45 crude extract, followed by assaying $C_2H_2$ reduction as described previously.[26] The activity results listed in Table I are the means of triplicate determinations with standard deviations of 6–11%. The "before" samples were stored in dry ice for the duration of the experimental runs, and all activity measurements were performed concurrently with the same *Av* UW45 extract.

**3. Sample Integrity and Preparation for XAS Data Acquisition.** All samples were thawed in a Vacuum Atmospheres inert-atmosphere box

(21) Abbreviations used: EPR, electron paramagnetic resonance; EXAFS, extended X-ray absorption fine structure; XAS, X-ray absorption spectroscopy; XANES, X-ray absorption near edge structure; *Av*, *Azotobacter vinelandii*; *Cp*, *Clostridium pasteurianum*.

(22) (a) Cramer, S. P.; Hodgson, K. O. *Prog. Inorg. Chem.* **1979**, *25*, 1 and references therein. (b) Lee, P. A.; Citrin, P. H.; Eisenberger, P.; Kincaid, B. M. *Rev. Mod. Phys.* **1981**, *53*, 769 and references therein.

(23) Conradson, S. D.; Burgess, B. K.; Newton, W. E.; McDonald, J. W.; Rubinson, J. F.; Gheller, S. F.; Mortenson, L. E.; Adams, M. W. W.; Mascharak, P. K.; Armstrong, W. A.; Holm, R. H.; Hodgson, K. O. *J. Am. Chem. Soc.* **1985**, *107*, 7935.

(24) Mortenson, L. E. *Methods Enzymol.* **1972**, *29*, 446.

(25) Mortenson, L. E.; Walker, M. W.; Walker, G. A. In *Proceedings of the International Symposium on Nitrogen Fixation, 1st, 1974*; Newton, W. E., Nyman, C. J., Eds.; Washington State University Pullman, WA, 1976; p 117.

(26) Burgess, B. K.; Jacobs, D. B.; Stiefel, E. I. *Biochim. Biophys. Acta* **1980**, *614*, 196.

(27) Diehl, H.; Smith, G. F.; McBride, L.; Cryberg, R. *The Iron Reagents*; G. Fredrick Smith Chemical Co.: Columbus, OH, 1965; p 1.

(28) Clark, L. J.; Axley, J. H. *Anal. Chem.* **1955**, *27*, 2000.

(containing $N_2$) and transferred by syringe to XAS cells, which had been previously rinsed within the glovebox with the appropriate solvent ($H_2O$ or NMF) containing 1.2 mM $Na_2S_2O_4$. Following the XAS experiments, the samples were unloaded in the same glovebox and transferred to serum vials, which were stored frozen in dry ice until assayed. In addition to reconstitution activity measurements, EPR spectra were recorded for each FeMo-co sample before *and* after the XAS experimental runs. All samples exhibited the appropriate EPR signal, which was unchanged by the data collection. There was no obvious difference in the EPR spectra from PhSH- and PhSeH-treated FeMo-co solutions, both of which showed identical sharpening of all three components of the signal.[18,19,23]

Sample integrity during data acquisition was maintained by the use of cells fabricated to be airtight to prevent exposure to $O_2$. The nylon cells contained the solution in a rectangular volume with thin walls both on the sides and top to allow maximum transmission of the incoming beam and the outgoing fluorescence signal, which is detected normal to the incoming beam direction. The cell volume was 1200 $\mu$L, the length of the transmission path was 20 mm, the width of the enclosed volume was 20 mm, and the height was 3 mm. The design maximized the fraction of the sample fluorescence reaching the detectors and permitted the sample to contact only Au, nylon, Viton, and Teflon, all of which were inert to the solvent systems and protein or cofactor. The sample cell was enclosed in a second airtight box with Mylar windows, through which a constant flow of He or $N_2$ was maintained throughout the course of the experiments. Sample temperature was controlled by a thermoelectric cooling module and monitored by an Fe-constantan thermocouple calibrated at 0 °C. MoFe protein samples were maintained between 2 and 4 °C and all FeMo-co samples between −15 and −25 °C to increase stability. The success of these sample-handling procedures is evident in that losses of activity averaged only 5% and were at most 15%.

**4. Sample Oxidation State.** It has been reported that during the course of XAS data acquisition solvated electrons are produced and that these electrons can cause appreciable reduction of some metalloproteins.[29] Our EPR data demonstrate that all of our samples were in the semireduced redox state at the onset of every experiment, and that they were in the same state after the samples were recovered from the XAS cells (following ~15 h of X-ray exposure). Although we cannot experimentally eliminate the possibility that reduction occurred during the course of the measurements, this would seem highly unlikely, since in all in vitro systems the reduction of the MoFe protein requires reduced Fe protein and MgATP. Thus, the effectiveness of radiolysis products in reducing protein-bound FeMo-co may be quite low. If reduction did occur, the MoFe protein and, by analogy, isolated FeMo-co should rapidly reoxidize by evolving $H_2$ from $H_2O$. Although it is possible that significant amounts of the relatively stable one electron/FeMo-co reduced state of the MoFe protein were produced and then reoxidized during subsequent sample transfers, it is, overall, quite unlikely that sample heterogeneity caused by reduced states is a problem with these data.

**5. Data Acquisition Conditions.** All data were acquired at SSRL under dedicated operation on wiggler end station 4-2. About 20–25 complete 25–35-min data scans were collected on each sample, for a total acquisition time of 10–12 h. Si(220) crystals were used in the monochromator. Problems related to the harmonic content of the monochromatized X-ray beam are small at these high photon energies (>20 keV) because of the rapid falloff in the spectral distribution of the synchrotron radiation. Nevertheless, the monochromator crystals were detuned by adjusting the Bragg angle of one crystal relative to the other until the ion chamber current was about half the maximum, thereby further minimizing the harmonic content of the X-ray beam.

The experimental setup consisted of, in order, adjustable slits, monochromator, adjustable slits, first ion chamber (incident intensity monitor), sample, second ion chamber (sample transmission monitor), Mo foil calibration standard, and a third ion chamber (calibration standard transmission intensity monitor). Data for the as-isolated FeMo-co sample 4 were recorded without the calibration standard and third ion chamber. Because of the low (0.5–1.3 mM) Mo concentrations, sample absorbances were determined as described previously by measuring the Mo K fluorescence with an array of NaI(Tl) scintillation detectors.[30]

**6. Data Analysis.** Data were analyzed by the procedures previously described.[31-33] Calibrations were performed for each scan with the Mo foil between the second and third ion chambers or, for sample 4, by means of periodically measuring the spectrum of a Mo foil substituted for the sample. The first inflection point in the Mo foil edge absorption spectrum was defined as 20 003.9 eV. The threshold energy ($E_0$) was defined as 20 025 eV. Both values are consistent with earlier work,[16,33b] which allows the application of the same curve-fitting parameter sets (the S1 set) used previously.[16,32,33b]

The data from each detector were recorded and analyzed separately to ensure that anomalies resulting from the effects of the relative positions of the incident beam, the sample, and the detector would not affect the final data. Thus, after calibration, for each scan from a particular detector, the absorbance and weighting factor were calculated and normalized so that the difference in absorbance between the extrapolated preedge and a minus third-order polynomial fit to the EXAFS region was defined as 1 at $E_0$. The individual scans were then inspected, and if obvious problems were observed, the affected points were either corrected, removed, or the data from that scan were not included in the average.

The types, numbers, and Mo-scatterer distances of the atoms in the various scattering shells were determined by curve fitting the EXAFS using modeled waves defined by a parametric equation and empirically derived curve-fitting parameters as described previously.[33] In addition to performing curve fits on the Fourier-filtered data, the raw (unfiltered) EXAFS from MoFe protein sample 2 was curve fit directly. No significant differences in the values calculated by fitting unfiltered relative to Fourier-filtered data were observed. Details of the different curve-fitting parameter sets and their derivations will be described elsewhere.[32]

Curve fits of the EXAFS from samples 1, 2, 4, 5, and 7–9 were performed over the range $k$ = 4–16 Å$^{-1}$. Curve fits over a shorter range, $k$ = 4–14 Å$^{-1}$, were performed on the EXAFS from samples 3 and 6, since these data did not extend as far. Curve fits over this shorter range were also performed on the EXAFS from samples 1 and 4 to determine any fitting-range-dependent corrections to the calculated distances and numbers. Because the data from samples 3 and 6 were available over only the shorter range, the results of these fits are used only as confirmation of the results from the fits over the longer range and are not relied upon as a basis for the determination of the numbers reported in Table IV. It should also be noted that curve-fitting analysis as described herein is unable to distinguish between elements adjacent in atomic number.[22] The "O" atoms calculated by the fit could also conceivably be N or C atoms and the "S" atoms could be Cl, all of which are present in these samples.

The effects of the background subtraction and Fourier-filtering procedures on the Mo-scatterer distances and scatterer numbers determined from the curve fits were examined by performing multiple fits on EXAFS calculated by using different background and filtering parameters. Because of the time required to apply this procedure, it was performed for each sample but only for the three-wave curve fits using the O2, S1, and Fe1 parameter sets. Subsequently, from this set of curve fits for each sample, one spectrum out of the set calculated with different background subtraction and Fourier-filtering parameters was selected, giving preference based on both good correspondence of the fit to the data (low sum of the squares of the residuals) and values that were close to the averages of all the fits and not the extremes. All other types of curve fits, the three-wave fits using waves generated from the S1, S1 and Fe1, and the O2, S1, and Fe2 parameter sets, and the four-wave fits, were then performed only once for each sample, using this same determination of the EXAFS. These spectra were also used as the basis for the figures. The origins of all the different curve-fitting parameter sets will be described in another paper, and the labels of these parameter sets have been retained.[32]

## Results and Discussion

Direct comparison of background-subtracted, normalized EXAFS spectra offers the simplest way to obtain a qualitative measure of structural differences between samples. The technique of Fourier transformation provides more detail in terms of different distances and, to a lower degree of accuracy, coordination numbers.[22] The most reliable approach to obtaining metrical information on these systems with multiple coordination shells is by far that of numerical analysis by curve fitting.[22,34] In the following section, the EXAFS results on the MoFe component of nitrogenase

(29) (a) Powers, L.; Blumberg, W. E.; Chance, B.; Barlow, C. H.; Leigh, J.; Smith, J.; Yonetani, T.; Vik, S.; Peisach, J. *Biochim. Biophys. Acta* **1979**, *546*, 520. (b) Chance, B.; Pennie, W.; Carman, M.; Legallais, V.; Powers, L. *Anal. Biochem.* **1982**, *124*, 248.

(30) (a) Jaklevic, J.; Kirby, T. A.; Klein, M. P.; Robertson, A. S.; Brown, G. S.; Eisenberger, P. *Solid State Commun.* **1977**, *23*, 679. (b) Cramer, S. P.; Scott, R. A. *Rev. Sci. Instrum.* **1981**, *52*, 395. (c) Stern, E. A.; Heald, S. M. *Rev. Sci. Instrum.* **1979**, *50*, 1579.

(31) Penner-Hahn, J. E.; Hodgson, K. O. *Phys. Bioinorg. Chem. Ser.*, in press.

(32) Conradson, S. D. Ph.D. Thesis, Stanford University, 1983; manuscript in preparation.

(33) (a) Cramer, S. P.; Hodgson, K. O.; Stiefel, E. I.; Newton, W. E. *J. Am. Chem. Soc.* **1978**, *100*, 2748. (b) Cramer, S. P. Ph.D. Thesis, Stanford University, 1977. (c) Eccles, T. K. Ph.D. Thesis, Stanford University, 1977.

(34) Berg, J. M.; Hodgson, K. O.; Cramer, S. P.; Corbin, J. L.; Elsberry, A.; Pariyadath, N.; Stiefel, E. I. *J. Am. Chem. Soc.* **1979**, *101*, 2774.

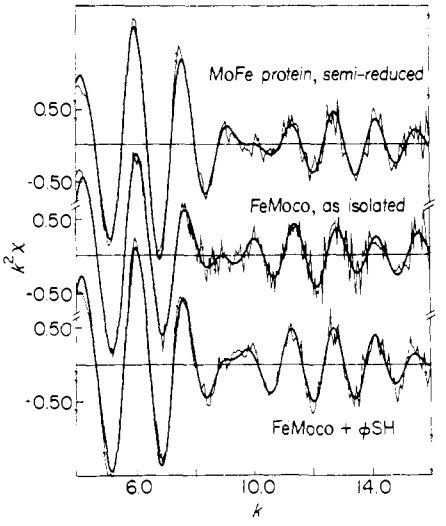


**Figure 1.** EXAFS data $k^2$ weighted of nitrogenase (from top to bottom): semireduced MoFe protein sample 1; as-isolated FeMo-co sample 4; FeMo-co + PhSH sample 7. The light lines are the actual data, and the dark lines are derived by Fourier filtering over a wide $R$ range to facilitate visual comparisons.

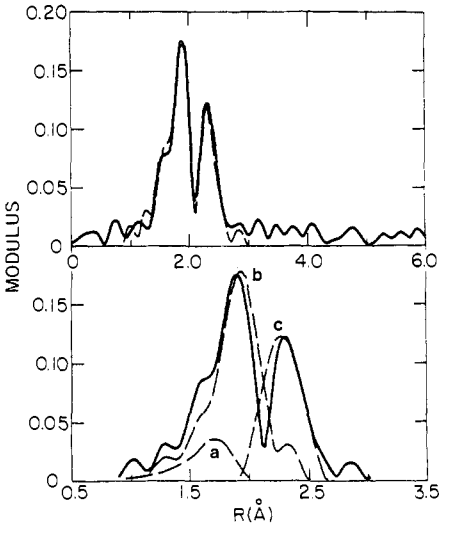


**Figure 2.** Top: (—) Fourier transform modulus of EXAFS of semireduced MoFe protein sample 1; (---) Fourier transform modulus of the total three-wave fit to the Fourier-filtered EXAFS of semireduced MoFe protein sample 1 using the O2, S1, and Fe1 parameter sets. Bottom: (—) Fourier transform modulus of the total three-wave fit to the Fourier-filtered EXAFS of semireduced MoFe protein sample 1 using the O2, S1, and Fe1 parameter sets; (---) Fourier transform modulis of the individual components of this three-wave fit, (a) the Mo–O wave calculated with the O2 parameter set, (b) the Mo–S wave calculated with the S1 parameter set, (c) the Mo–Fe wave calculated with the Fe1 parameter set. Transforming and fitting range is $k$ = 4–16 Å$^{-1}$.

and the FeMo-co are analyzed from each of these three viewpoints.

**1. Data Quality and Qualitative Comparisons.** The EXAFS of the semireduced MoFe protein (sample 1), FeMo-co (sample 4), and FeMo-co with added PhSH (sample 7) are presented for comparison in Figure 1, and the Fourier transform moduli of these data, together with that for FeMo-co + PhSeH (sample 9) in Figure 2–5. The data are characterized by low noise levels even up to high $k$ values of 16–17 Å$^{-1}$. This extended data range provides the opportunity for more accurate analyses of the EXAFS than was available in our earlier work.[16a,b]

The overall similarity in amplitude and phase at both low and high $k$ for all of the nine samples studied (only the data for three are shown in Figure 1) provides evidence that certain coordination features are common to all of the protein and FeMo-co samples. Earlier work[16a,b] indicated that the features dominating the EXAFS spectrum were due to the presence of two strongly scattering

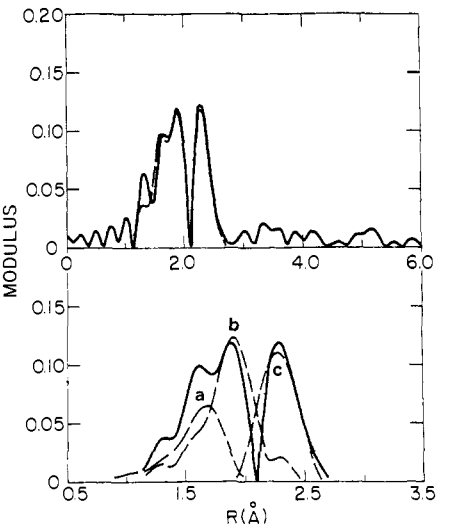


**Figure 3.** Top: (—) Fourier transform modulus of EXAFS of as-isolated FeMo-co sample 4; (---) Fourier transform modulus of the total three-wave fit to the Fourier-filtered EXAFS of as-isolated FeMo-co sample 4 using the O2, S1 and Fe1 parameter sets. Bottom: (—) Fourier transform modulus of the total three-wave fit to the Fourier-filtered EXAFS of as-isolated FeMo-co sample 4 using the O2, S1 and Fe1 parameter sets; (---) Fourier transform moduli of the individual components of this three-wave fit, (a) the Mo–O wave calculated with the O2 parameter set, (b) the Mo–S wave calculated with the S1 parameter set, (c) the Mo–Fe wave calculated with the Fe1 parameter set. Transforming and fitting range is $k$ = 4–16 Å$^{-1}$.

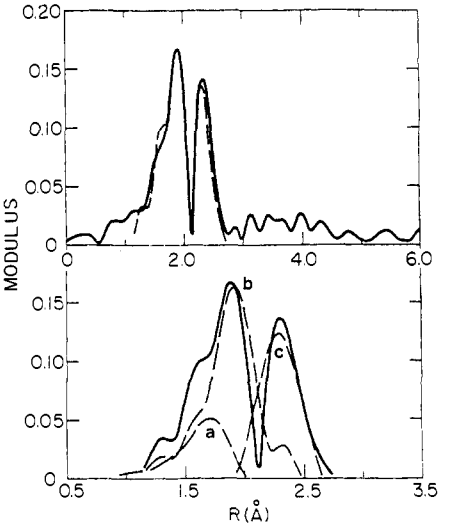


**Figure 4.** Top: (—) Fourier transform modulus of EXAFS of FeMo-co + PhSH sample 7; (---) Fourier transform modulus of the total three-wave fit to the Fourier-filtered EXAFS of FeMo-co + PhSH sample 7 using the O2, S1 and Fe1 parameter sets. Bottom: (—) Fourier transform modulus of the total three-wave fit to the Fourier-filtered EXAFS of FeMo-co + PhSH sample 7 using the O2, S1 and Fe1 parameter sets; (---) Fourier transform moduli of the individual components of this three-wave fit, (a) the Mo–O wave calculated with the O2 parameter set, (b) the Mo–S wave calculated with the S1 parameter set, (c) the Mo–Fe wave calculated with the Fe1 parameter set. Transforming and fitting range is $k$ = 4–16 Å$^{-1}$.

shells of atoms, one of sulfur and one of iron. Small differences in the amplitudes and significant differences in the beat region from $k$ = 8–11 Å$^{-1}$ (the point where the different frequency components are strongly interfering) suggest the presence of a third shell of atoms as well as possible variation of the numbers of atoms in the first two shells.

Striking visual differences in the shape of the amplitude envelope in the beat region of the different sample types are easily observed. The shape of the amplitude envelope in terms of the absolute and relative magnitudes of the oscillations near $k$ = 8, 9, and 10 Å$^{-1}$

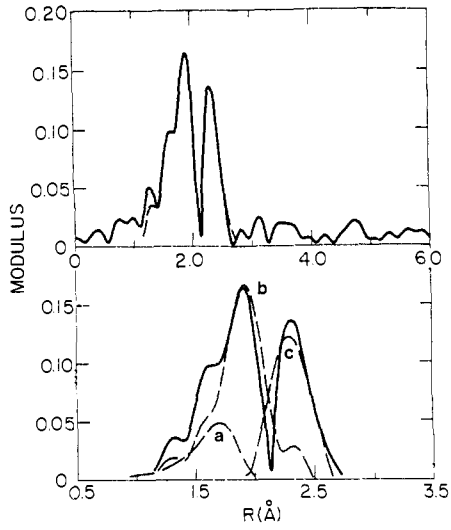


**Figure 5.** Top: (—) Fourier transform modulus of EXAFS of FeMo-co + PhSeH sample 9; (---) Fourier transform modulus of the total three-wave fit to the Fourier-filtered EXAFS of FeMo-co + PhSeH sample 9 using the O2, S1 and Fe1 parameter sets. Bottom: (—) Fourier transform modulus of the total three-wave fit to the Fourier-filtered EXAFS of FeMo-co + PhSeH sample 9 using the O2, S1 and Fe1 parameter sets; (---) Fourier transform moduli of the individual components of this three-wave fit, (a) the Mo–O wave calculated with the O2 parameter set, (b) the Mo–S wave calculated with the S1 parameter set, (c) the Mo–Fe wave calculated with the Fe1 parameter set. Transforming and fitting range is $k$ = 4–16 Å$^{-1}$.

for the MoFe protein sample is opposite to that found for both types of FeMo-co samples. This specific difference in the appearance of the EXAFS occurs in all the data sets collected for these samples and for all variations of the background and Fourier filter parameters.

These differences are clearly indicative of a change in the Mo environment upon removal of FeMo-co from the protein and upon subsequent addition of PhSH/PhSeH. In contrast, the data from the FeMo-co + PhSH sample 7 and FeMo-co + PhSeH sample 9 (not shown) are virtually superimposable, indicating that, at least at this level of examination, the structures of their Mo sites are the same. Thus, the Se of the PhSeH and, by analogy, the S of the PhSH do not bind to the Mo atom, corroborating the results of Mascharak et al.[35] and our results from study of the XANES region.[23]

**2. Comparison of Fourier Transforms.** Fourier transforms (FTs) of EXAFS data provide information on the major frequency components that constitute the spectrum. As such, FTs are frequently used for visual comparisons and for determining starting values for the more accurate analysis by curve fitting. The FTs of multiple-shell systems cannot account for the phase shift in EXAFS data, and thus true distances not obtained directly. In general, the peaks in a FT of EXAFS data are shifted to lower $R$,[22] and estimates of the true interatomic distances can be obtained by adding about 0.35–0.4 Å to the observed peak positions.

As seen from visual comparisons among Figures 2–5, all of the transforms show the two major frequency components that have been attributed to Mo–S and Mo–Fe scattering shells. The most obvious difference among the transforms shown is in the first peak around 1.9 Å for FeMo-co (Figure 3) when compared with any of the other transforms. The transforms for semireduced MoFe protein, FeMo-co + PhSH, and FeMo-co PhSeH are more similar to each other.

Some further suggestions about the Mo coordination environment can be gained by comparison of the protein and FeMo-co transforms with relevant synthetic model complexes. For example, the Fourier transform moduli of the EXAFS from FeMo-co (sample 4) and FeMo-co + PhSH (sample 8) are distinctly similar in appearance to those from synthetic compounds containing cubane-type $MoFe_3(\mu_3\text{-}S)_4$ cores with anionic O atoms as nearest neighbors to the Mo atom.[32] The origins of the three principal features in the data from the model complexes are the shells of O, S, and Fe atoms. The data from FeMo-co + PhSH/PhSeH samples 7 and 9) and from the semireduced MoFe protein do not exhibit a resolved peak at $R$ = 1.60–1.65 Å and most closely resemble in appearance the data from one sample of $(Et_4N)_3[MoFe_3S_4(SEt)_3(cat)_3]$.[32]

The analogies in the appearance of the data and FTs suggest the presence of a $MoFe_xS_yO_z$ coordination unit with Mo–O distances of ~2.1 Å, Mo–S distances of ~2.35 Å, and Mo–Fe distances of ~2.7 Å in each of these nitrogenase and FeMo-co sample types. Also, no features beyond $R$ = 2.3 Å, which would result from ordered shells of atoms farther than 2.7 Å from the Mo atom, are observed in the FT moduli. By analogy with observations in the data from synthetic compounds, any more distant Fe, Se, or Mo atoms or shells of low $Z$ atoms must be more distant from the Mo atom than approximately 3.5–4.0 Å.

**3. Numerical Results from Curve-Fitting Analyses.** Least-squares curve fitting currently offers the most accurate way to obtain metrical information from the EXAFS data on the Mo site in the protein and cofactor.[22,31,33] As described previously in detail, the curve-fitting procedure depends on fitting a model of the phase and amplitude of each coordinating shell type to the unknown while varying parameters, in this case the distance to and number of coordinating atoms in each shell. Amplitude and phase functions may be calculated ab initio[36] or determined semiempirically from model complexes of known structure.[22] For reasons we have described in detail in the literature,[16,22] the latter approach has been utilized for fitting Mo in the work described herein. In complex multiple coordination shell environments such as those found in the Mo–Fe–S clusters, we have found it is not possible because of parameter correlation to do multiple shell fits (three or more shells) where both the relative Debye–Waller factors and the coordination numbers are varied. Thus, in the approach used herein, changes in relative Debeye–Waller factor are reflected in errors in coordination number. From studying a large number of (greater than 25) molybdenum model compounds of known structure using this approach, the accuracy of distances and coordination numbers have been shown to be around ±0.02 Å in distance and within 25% in coordination number.[16,22,33,34] Specific examples relevant to the Mo–Fe–S systems under study herein will be considered as appropriate below.

**(a) Amplitude and Phase Parameter Sets.** One of the problems inherent to curve-fitting analyses is the transferability of the phases and amplitudes from the model to the unknown.[22] We minimize errors introduced by any lack of transferability by using empirical waves, which were derived, refined, and tested by using the EXAFS from a large number of structurally analogous synthetic compounds with known structures.[32] The Mo–O parameter set (called O2) was obtained from the EXAFS of $Mo(acac)_3$. The EXAFS of $Mo(S_2C_6H_4)_3$ was used to determine the Mo–S parameter set (called S1). For Mo–Fe parameter sets, we found that two different parameter sets were needed to cover optimally all the different models.

The Fe1 parameters were derived from the Fourier-filtered Mo–Fe wave of the EXAFS from FeMo-co sample 4. Initial trial parameters were obtained from sample 4, and then the per atom amplitude and the linear phase shift were optimized from curve fits of the EXAFS from compounds with known structures possessing the $MoFe_3(\mu_3\text{-}S)_3(\mu\text{-}S)_3$ coordination unit.[32] The validity of this procedure was established by the accuracy of the metrical information obtained from curve fits of the EXAFS of a large number of other model complexes with known structures, as will be described in detail elsewhere.[32] The Fe2 parameter set was derived from the Fe1 set by increasing the exponential damping factor to optimize the accuracy in the calculated number of Fe atoms and enhance the quality of curve fits of the EXAFS from

(35) Mascharak, P. K.; Smith, M. C.; Armstron, W. H.; Burgess, B. K.; Holm, R. H. *Proc. Natl. Acad. Sci. U.S.A.* **1982**, *79*, 7056.

(36) (a) Lee, P. A.; Teo, B.-K.; Simons, A. L. *J. Am. Chem. Soc.* **1977**, *99*, 3856. (b) Teo, B.-K. Lee, P. A. *J. Am. Chem. Soc.* **1979**, *101*, 2815.

**Table II.** Results of Three-Wave Curve Fits Using the S1, S1, and Fe1 Parameter Sets

| | closer S shell | | outer S shell | | Fe shell | | $\sum$(fit data)$^2$ | |
|---|---|---|---|---|---|---|---|---|
| sample no. | dist, Å | no. of atoms | dist, Å | no. of atoms | dist, Å | no. of atoms | abs | rel[a] |
| 1 | 2.278 | 1.40 | 2.379 | 4.75 | 2.680 | 3.55 | 0.60 | 1.18 |
| 2 | 2.277 | 1.52 | 2.381 | 4.78 | 2.682 | 3.58 | 0.59 | 0.91 |
| 4 | 2.264 | 2.44 | 2.379 | 3.29 | 2.682 | 3.01 | 0.80 | 1.40 |
| 5 | 2.249 | 2.08 | 2.381 | 3.30 | 2.715 | 2.43 | 0.56 | 1.45 |
| 7 | 2.289 | 2.21 | 2.384 | 4.14 | 2.698 | 3.64 | 0.58 | 1.12 |
| 8 | 2.254 | 1.74 | 2.380 | 4.54 | 2.707 | 3.39 | 0.74 | 1.83 |
| 9 | 2.271 | 1.67 | 2.376 | 4.54 | 2.697 | 3.58 | 0.62 | 1.36 |

[a] Relative to fits with the O2,S1,Fe1 parameter set reported in Table III. For fits of equal overall quality, the ratio would be 1, and the larger the number, the poorer the fit for the S1,S1,Fe1 parameter set.

**Table III.** Results and Reproducibility Comparisons of Three-Wave Curve Fits Using the O2, S1 and Fe1 Parameter Sets

| | O shell | | S shell | | Fe shell | |
|---|---|---|---|---|---|---|
| sample | dist, Å | no. of atoms | dist, Å | no. of atoms | dist, Å | no. of atoms |
| semireduced MoFe protein | | | | | | |
| 1 | 2.116 | 1.60 | 2.367 | 4.51 | 2.676 | 3.49 |
| 2 | 2.117 | 1.72 | 2.369 | 4.43 | 2.678 | 3.47 |
| 3[a] | 2.138 | 0.99 | 2.366 | 4.65 | 2.682 | 3.61 |
| variation within same run | 0.001 | 0.12/1.66 (7%) | 0.002 | 0.08/4.47 (2%) | 0.002 | 0.06/3.46 (2%) |
| variation for different runs | 0.018 | 0.67/1.33 (50%) | 0.002 | 0.18/4.56 (4%) | 0.005 | 0.15/3.54 (4%) |
| as-isolated FeMo-co | | | | | | |
| 4 | 2.092 | 2.93 | 2.348 | 2.99 | 2.677 | 2.98 |
| 5 | 2.102 | 3.31 | 2.385 | 3.15 | 2.716 | 2.28 |
| 6[a] | 2.117 | 3.47 | 2.374 | 3.44 | 2.703 | 3.00 |
| variation for different runs | 0.025 | 0.54/3.24 (17%) | 0.037 | 0.45/3.19 (14%) | 0.039 | 0.72/2.75 (26%) |
| FeMo-co + PhSH/PhSeH | | | | | | |
| 7 | 2.117 | 2.51 | 2.364 | 4.08 | 2.695 | 3.40 |
| 8 | 2.107 | 3.00 | 2.372 | 3.70 | 2.707 | 3.16 |
| 9 | 2.107 | 2.43 | 2.364 | 4.19 | 2.695 | 3.41 |
| variation within same run | 0.010 | 0.08/2.47 (3%) | 0 | 0.11/4.13 (3%) | 0 | 0.01/3.40 (0%) |
| variation for different runs | 0.005 | 0.53/2.74 (19%) | 0.008 | 0.43/3.91 (11%) | 0.012 | 0.24/3.28 (7%) |

[a] As discussed in the Experimental Section, fits for these samples were over a more limited data range ($k$ = 4–14 Å$^{-1}$).

compounds possessing the $MoFe_3(\mu_3\text{-}S)_3O_3$ coordination unit.

The quality of fits and derived distances for the protein and cofactor samples using either Fe1 or Fe2 parameter sets were found to be essentially the same. The number of Fe atoms calculated from fits with the Fe2 parameters were an average of about 25% higher than for those fits using the Fe1 parameters. The relevance of this to the number of iron atoms in the samples is discussed in more detail in section 3c. Given the satisfactory fits using the Fe1 set to many model complexes with the Mo–Fe–S core,[32] and in the absence of information suggesting that the Fe2 parameter set is preferable, we have used the Fe1 set in the curve fits described later.

**(b) Three-Wave Fits. S–S′–Fe Versus O–S–Fe.** The proposed structures of the Mo site, based on the original interpretations of the first EXAFS data, postulate, in addition to Fe, either only S ligation or primarily S with the possibility of one other atom of a different type.[16a,b] Given the much improved quality and range of our data and the subsequent existence of a large number of structurally analogous synthetic compounds whose EXAFS provide a means for testing the curve-parameter sets, the nature of the three shells around Mo can now be addressed more reliably. Three-wave curve fits utilizing two waves modeled by the S1 parameter set and one modeled by the Fe1 set were performed on all data sets, and the results are given in Table II. Comparable three-wave fits utilizing the O2, S1, and Fe1 parameter sets were also performed, and the results are given in Table III.

A significant decrease in the quality of the S1–S1–Fe1 fit relative to the O2–S1–Fe1 fit occurs for the data from FeMo-co (samples 4 and 5) and for FeMo-co + PhSH/PhSeH (samples 7–9). On the basis of these observations as well as the qualitative analyses of the XANES[23] and the EXAFS, it is most unlikely that the S–(S′)–Fe description of the Mo environment is correct for either of these sample types.

The curve fits of the MoFe protein data (samples 1–3) do not provide a basis for preferring either the S–S′–Fe or O–S–Fe configuration, since both are of comparable quality and either interpretation is chemically reasonable. The XANES, however, is unambiguously consistent only with the O–S–Fe structure.[23] In addition, a substantially larger rearrangement of the Mo site is required in the interconversion of protein-bound and free FeMo-co if the S–S′–Fe configuration occurs in the protein. It is, thus, also likely that the S–S′–Fe configuration is not present in the MoFe protein.

These conclusions differ in some details from those based on the original analyses[16a,b,d] of the EXAFS data. However, because a basis of structurally characterized compounds containing $Mo_xFe_yS_z$ clusters was not available at that time, the curve-fitting parameter sets used in the original analyses could not be refined or even tested. Curve fits of this original, lower quality data, using the methods described herein, produce results fully consistent with these more recent results.

**(c) Results from Three-Wave Curve Fits with the O2, S1, and Fe1 Parameter Sets.** The agreement between the calculated EXAFS and the data is overall very good as illustrated in the FTs (Figures 2–5) for the semireduced protein sample 1, the FeMo-co sample 4, and FeMo-co + PhSH/PhSeH (samples 7 and 9). As observed with fits to the model compounds having the $MoFe_3(\mu_3\text{-}S)_3O_3$ coordination unit,[32] the data exhibit the greatest variation, and the curve fits and the data differ most in the low $R$ region (1.4–1.7 Å). In the models, this appears to occur because the modulus peak of the Mo–O wave overlaps with the steeply rising portion of the modulus from the Mo–S wave. A similar explanation likely applies to the biological samples. The quantitative results for the O2–S1–Fe1 curve fits for each of the samples are summarized in Table IV.

**Errors in Data Processing and Analysis.** A systematic effort has been made to evaluate the reliability of the results for the O2–S1–Fe1 fits and to evaluate the effects of errors that might have been introduced either during data collection or from data reduction. The more subjective procedures in the data reduction process involve selecting the parameters that determine the polynomial spline background removal function and those chosen for the FT windows. To evaluate the effects of these two factors on the numerical results, we curve fit each data set several times

**Table IV.** Average Results[a] on the Mo Sites in the Semireduced MoFe Protein, As-Isolated FeMo-co, and FeMo-co + PhSH/PhSeH

| | O shell | | S shell | | Fe shell | |
|---|---|---|---|---|---|---|
| | Mo–O dist, Å | no. of atoms | Mo–S dist, Å | no. of atoms | Mo–Fe dist, Å | no. of atoms |
| semireduced MoFe protein | 2.12 ± 0.01 | 1.7 | 2.37 ± 0.01 | 4.5 | 2.68 ± 0.01 | 3.5 |
| as-isolated FeMo-co | 2.10 ± 0.02 | 3.1 | 2.37 ± 0.02 | 3.1 | 2.70 ± 0.02 | 2.6 |
| FeMo-co + PhSH/PhSeH | 2.11 ± 0.01 | 2.6 | 2.37 ± 0.01 | 4.0 | 2.70 ± 0.01 | 3.3 |

[a] The uncertainties in the distances are not a standard deviation, variance, or other statistical measure but are selected such that the distance ± the uncertainty encompasses the distances calculated from the curve fits of the EXAFS from all the samples of that particular state. (See the text for a more complete discussion of this.) Uncertainties in the numbers are discussed in detail in the text.

(typically 5–10) using EXAFS calculated with different background and Fourier-filtering parameters. For the S and Fe shells that contribute most significantly to the EXAFS, the average variation in distance was ±0.002 Å and ±0.1 atom in number. The O shell had a higher variation of ±0.01 Å in distance and ±0.3 atom.

The other measure of reliability is found in comparisons of the same sample type measured within the same or in different experimental runs. These results for the O2–S1–Fe1 fits are summarized in Table III. The variations for the Mo–X distances were on average about ±0.01 Å, although there were cases for S and Fe shells (samples 4–6) where the variations were ±0.02 Å. The average variation in coordination number was about 12%, but in one case (the O shell for samples 1–3), it was as large as 50%.

**Mo-Scatterer Distances.** The Mo-scatterer distances from the O2–S1–Fe1 curve fits (Table IV) are the averages of the curve-fitting results for all the samples of each given state. The reported uncertainties are determined by including the variations in the results from all the samples of a given sample type.

The largest variations are in the Mo–S and Mo–Fe distances calculated from the data of FeMo-co sample 4, which are 0.037 and 0.039 Å less, respectively, than those from sample 5 (Table III). These variations are an order of magnitude greater than those that result from using different background subtraction and Fourier-filtering processes (as described earlier) and are significantly larger than the 0.01–0.02-Å variations of this type that occur with the data from the model compounds. However, an uncertainty of ±0.02 Å does not affect the interpretation of these distances in terms of particular modes of bonding and structural moieties. We, therefore, find this slightly worse than expected level of precision acceptable. The variations in all the other distances are less than 0.02 Å. The Mo–O distances may be subject to a systematic error that is observed with the models[32] when Mo–O distances are >2.10 Å, and thus the actual distances may be 0.01–0.04 Å longer than the values determined here. The analyses of the data from models suggest no additional systematic errors of this sort.

From the results given in Table IV it is clear that the final Mo–X atom distances are the same within error limits for all the protein and FeMo-co samples. The structural differences inferred from qualitative comparisons of the EXAFS from these different samples must, therefore, originate in the *numbers* of atoms in the three shells around the Mo and *not* in their *distances* from the Mo.

**Coordination Numbers of Mo.** In the approach that we have developed and tested for curve-fitting EXAFS data, the numbers of atoms calculated are not constrained to integer values. While there are alternative approaches,[36,37] extensive studies of model systems with multiple ligand shells have shown this approach to be as or more reliable than fixing numbers and floating other parameters, such as the Debye–Waller factor.[16,31–33] If noninteger values arise, the problem is to deduce the best integer value (using other information where available). This difficulty occurs for the number of S atoms for the MoFe protein and the number of Fe atoms for all samples studied.

The number of O atoms calculated from the EXAFS of MoFe protein samples 1 and 2 (from *C. pasteurianum*) is 0.7 atom greater than that calculated for sample 3 (from *A. vinelandii*). It is unlikely, based on other physical evidence (including XANES results[23]), that the O shell is composed only of a single atom. This 50% variation in the calculated number of O atoms is not particularly surprising because of the low amplitude of the Mo–O wave relative to the Mo–S and Mo–Fe and because of the similarity in distances of the Mo–O and Mo–S waves that make contributions to the EXAFS. Because of these problems, as well as the effects of background residuals, the low $R$ region where the O shell makes its contribution is in general the area of poorest correspondence between the fit and the data, of both the models[32] and of these samples (Figures 2a–5a). This variation in number of O atoms may also be enhanced by experimental factors, since it is observed that the number of O atoms calculated by curve fitting the EXAFS of samples 1, 2, 7, and 9 (all acquired during experimental session A) are 14–20% lower than the next highest integer. The average number of O atoms for samples 1 and 2 (the two protein samples fit over the wide $k$ range) is 1.7.

From the curve fits of the EXAFS of FeMo-co samples 4 and 5, the calculated average number of O atoms proximal to the Mo atom is 3.1. The number of O atoms for sample 6 is 12% higher than the number from the other two data sets. If this was a real difference resulting from the HCl/NaOH isolation procedure used to prepare sample 6, it would be expected that the number of apparent O atoms would *decrease* as a citrate or phosphate O atom was replaced by $Cl^-$, and as mentioned before, this data set for 6 was available only over a more limited $k$ range. There is no significant indication that the number of O atoms is different from three in FeMo-co.

The number of O atoms calculated from the data sets of samples 7 and 9 (FeMo-co + PhSH/PhSeH) collected in experimental sessions A are midway between two and three, whereas the curve fit of the EXAFS of sample 8 gives exactly 3.0. Samples 7 and 9 are the other data sets from experimental session A that gave low numbers of O atoms. The 17% decrease in the calculated number of O atoms relative to the next highest integer (three) is within the expected error range. The number of oxygen atom nearest neighbors to the Mo in FeMo-co + PhSH/PhSeH thus appears to be three. If the oxygen shells in the FeMo-co and FeMo-co + PhSH/PhSeH samples are thus identical, the average number of oxygen atoms from all the samples is 2.8. This value is significantly higher than the value of 1.4 for the FeMo protein.

The calculated number of atoms in the S shell of the MoFe protein is also noninteger. There is no apparent experimental cause for the average value for samples 1, 2, and 3 of 4.53. Either four or five sulfur atoms could be accommodated. The effect could result from a fifth S atom (the first four being endogenous to the cofactor) being bound at a slightly different distance. This static disorder would result in a lower calculated number of atoms. In the absence of data from suitable known structures, the Mo X-ray absorption edge structure also does not preclude either the 2:5 or 2:4 O to S ratio.

In FeMo-co, the number of S atoms proximal to the Mo, as calculated from samples 4 and 5, deviates from three by 5% or less. The number of S atoms calculated from sample 6 is 13% higher than three. As with the oxygen case above, this difference is probably not significant because of the narrower range of fits in $k$ space for 6. Thus it is concluded that there are three sulfur atoms in the FeMo-co samples.

The numbers of S atoms neighbors around Mo calculated from the curve fits of the EXAFS from all FeMo-co + PhSH/PhSeH samples are consistent with the integer four (the average calculated number is 4.0). Thus, there is an additional S atom coordinated

(37) Antonio, M. R.; Teo, B.-K.; Cleland, W. F.; Averill, B. A. *J. Am. Chem. Soc.* **1983**, *105*, 3477.

to Mo in FeMo-co + PhSH/PhSeH relative to FeMo-co. This additional S atom does *not* arise from the PhSH, because no corresponding Mo–Se wave is observed in FeMo-co + PhSeH as described further in the discussion of four-shell fits. The increase in the number of S atoms is consistent with the difference in appearance of the EXAFS of FeMo-co compared with FeMo-co + PhSH/PhSeH.

Iron constitutes the third shell of atoms around Mo. The numbers of Fe atoms calculated for FeMo-co + PhSH/PhSeH samples 7 and 9 differ by only 2% from the values from MoFe protein samples 1 and 2 (all run during experimental session A). The values from other such samples run during other sessions are also in good agreement. Thus, the number of Fe atoms proximal to the Mo atoms is the same in the semireduced MoFe protein and FeMo-co + PhSH/PhSeH, with an average calculated value of 3.4. The average number of Fe atoms for the as-isolated FeMo-co samples is 2.6.

Besides contributions from experimental artifacts, nonintegral coordination numbers arise from Debye–Waller effects. If the distribution of Mo–Fe distances in the sample being studied is larger than that of the model from which the amplitude parameters were derived, a lower calculated coordination number will result. As discussed earlier, this was examined by fitting with a second set of Mo–Fe parameters (Fe2), with the result that the number of iron atoms increases by ~25%. For this Fe2 parameter set, the exponential damping factor is larger relative to the Fe1 set. It is, thus, very likely that the number of atoms in the Fe shell in the semireduced MoFe protein and FeMo-co + PhSH/PhSeH is four and that in the as-isolated FeMo-co is three, since smaller numbers require an exponential damping factor even less than that of the Fe1 parameter set.

The principal question is then whether the number of iron atoms in FeMo-co is significantly different from that in the protein and FeMo-co + PhSH/PhSeH. Unfortunately, this question cannot be answered definitively. The average calculated number of Fe atoms in the protein or in FeMo-co + PhSH/PhSeH is 31% greater (increase of 0.8 atom from 2.6 to 3.4) than in as-isolated FeMo-co. The largest error in the number of Fe atoms calculated from the EXAFS of eight model compounds containing $[MoFe_3S_4]$ clusters is 14%, and the average error is 6%.[32] The larger numbers of Fe atoms calculated from the EXAFS of the semireduced MoFe protein and FeMo-co + PhSH/PhSeH compared with FeMo-co itself are, therefore, in the range of being significant.

**(d) Results from Four-Wave Fits.** The other alternatives to the O–S–Fe configuration that should be considered are those containing more than three shells of nearest-neighbor atoms within 2.7 Å of the Mo atom. The analyses of the EXAFS from synthetic compounds containing $MoFe_3S_3O_3$, $MoFe_3S_3O_2C$, and $MoFe_3S_3S'O_2$ coordination units indicate that the curve-fitting procedure is unable to reliably determine the correct structure when more than three shells of nearest-neighbor atoms are present within 2.7 Å of the Mo atom.[32] It is also often unreliable in distinguishing whether three or more shells exist.

One set of meaningful four-wave curve fits assuming an Mo-$Fe_xS_yO_zSe$ configuration was performed on the EXAFS from FeMo-co + PhSH/PhSeH. Because all four of these waves are unique and are, therefore, less likely to correlate, these curve fits should be able to demonstrate whether the Se atom of PhSeH coordinates to the Mo atom in FeMo-co. All of these fits, including the two where Se is not present in the sample, calculated a fraction (around 0.3) of a Se atom, but with a large variation in the Mo–Se distance (2.48–2.6 Å). Therefore, assuming that the reaction of PhSeH with FeMo-co parallels that with PhSH, neither thiolate S nor selenide Se binds to the Mo atom. The additional S atom that appears in the Mo coordination sphere of FeMo-co in the presence of PhSH or PhSeH must, therefore, be endogenous to FeMo-co.

## Conclusions

On the basis of structurally analogous synthetic compounds, the observed Mo–O(N) distances are consistent with anionic ligands but are too short for neutral solvent molecules. The nature of these ligands is as yet unknown. Within the protein, the ligands aspartate, glutamate, tyrosinate, asparagine, and glutamine are possible.[38] In FeMo-co, which does not possess amino acids, it is conceivable that they could be oxo or hydroxo endogenous bridges to Fe atoms or that they could be exogenous, possibly citrate or phosphate (when present), dithionite, sulfite, hydroxide, or deprotonated NMF. In this regard, it is notable that FeMo-co is extracted by "basic" rather than "acidic" NMF,[10] which may be a requirement so that an anionic ligand (possibly deprotonated NMF itself) is available to replace those supplied by the protein matrix.

The Mo–S distances are consistent with bridging sulfides bound to hexacoordinate Mo, just as the Mo–Fe distances are within the range (although tending toward the short side) of sulfide-bridged Mo–Fe bonds. A minimal configuration of three S atoms and three Fe atoms at the appropriate distances probably occurs in all three of the protein and FeMo-co states studied. The $[MoFe_3S_4]$ cubane-type cores are the most stable arrangement of these atoms known, which also have the required stoichiometry and magnetic properties. However, the S atom at the vertex opposite the Mo in such a core is too distant to be observed, even with the highest quality data from the synthetic compounds.[32] The presence of the entire $[MoFe_3S_4]$ entity as a part of FeMo-co thus cannot be proven by XAS.

The distances from the Mo to the additional S and, possibly, Fe atoms that occur in the semireduced MoFe protein and FeMo-co + PhSH/PhSeH compared with FeMo-co are the same as those for the other atoms present. These similarities imply structural similarity; *i.e.*, these atoms also occur as bridging sulfide (although it is conceivable that this Mo–S distance could be that of a terminal thiolate) and as sulfide-bridged Fe, respectively. Because the Se of PhSeH does not bind to the Mo, these additional atoms must be endogenous to the protein or FeMo-co.

In addition to these comparisons with known compounds, the Mo environments deduced from these studies (Table IV) indicate two situations without precedent in any compound yet synthesized and characterized: (1) the number of O(N) + S nearest neighbors to the Mo in the three samples types is not constant and could be seven in one or two of the states; (2) the number of Fe atoms proximal to the Mo in the three sample types is also not constant and may be either three (in as isolated FeMo-co) or four (in protein and in FeMo-co + PhSH/PhSeH).

With regard to the number of O(N) + S nearest neighbors, one more observation is pertinent. Independent of these interpretations, based strictly on qualitative comparisons of the EXAFS and XANES, it appears certain that: (1) the local Mo environments in the three sample types are different; (2) at least two O(N) atom nearest neighbors occur in all samples; (3) at least three S atom nearest neighbors occur in all three sample types.

These radial structures at Mo are the first to be reported in detail for FeMo-co and FeMo-co + PhSH/PhSeH. The conclusions based on the EXAFS are consistent with the inferences drawn from our analyses of the XANES of these same samples.[23] The Mo environment described herein, however, differs in various ways from both the previously published Mo EXAFS studies[16a,b] and from the interpretation of the $^{95}Mo$ ENDOR spectra.[14] The early interpretation of the Mo EXAFS of the protein provided strong evidence for three to four sulfur atoms at ~2.35 Å from Mo and two to three iron atoms with a Mo–Fe distance of 2.72 Å.[16a] Of less certainty was the indication of another shell of one or two sulfur atoms at a larger distance. Our subsequent reanalysis of the same data led to the conclusion that the more distant S shell was an artifact. The closer S shell compares favorably in distance and number with the S shell that we find in this work of four or five atoms with a Mo–S distance of 2.37 Å. The differences with respect to the outer S shell and the Fe shell and the absence of any other shell are significant. As explained above, when these early EXAFS analyses were undertaken, no Mo–Fe containing compounds had been synthesized, and so an untested, simulated Mo–Fe wave had to be used to model the real one in

(38) Brigle, K.; Newton, W. E.; Dean, D. R. *Gene* **1985**, *37*, 37.

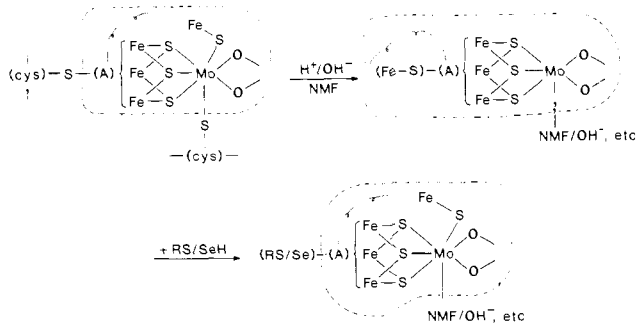


**Figure 6.** Possible structures and interconversion scheme of the Mo site in the semireduced MoFe protein, as isolated FeMo-co, and FeMo-co + PhSH/PhSeH based on the results of these studies. The dotted line signifies endogenous components; (A) is the remainder of the FeMo-co core; () represents XAS invisibility.

curve fits of the EXAFS of the semireduced MoFe protein. An artifact of the Mo–Fe wave used was the second S shell of 2.49 Å. The uncertainty associated with this outer S shell and the Fe shell was noted in the first of the previous analyses. Because we have now been able to extract and test an empirical Mo–Fe wave, we have overcome these problems and conclude that the long S shell does *not* exist and that a shell of a lower $Z$ atom (O, N, or C) does.

The variance with the conclusions from the $^{95}$Mo ENDOR study[14] is the same as that reached from our XANES data.[23] The EXAFS analyses are completely incompatible with a tetrahedral arrangement of nearest neighbors to the Mo, which is the geometry favored by the ENDOR interpretation. Both the EXAFS and absorption edge sources of data indicate geometries of significantly higher coordination number.

The fact that the first coordination sphere of the Mo in the semireduced MoFe protein differs from that in FeMo-co + PhSH/PhSeH suggests either that some of the Mo ligands are from the protein or that, even if they are not, the protein still influences the structure of FeMo-co so that additional S and Fe atoms from elsewhere within FeMo-co become bound to the Mo. If the number of atoms in the S shell in the semireduced MoFe protein is five, then possibly one protein thiolate (shown in Figure 6) binds to the Mo, which is replaced by $RO^-$ (or $RNH^-$) when FeMo-co is extracted. The additional S atom present in both FeMo-co + PhSH/PhSeH and the semireduced MoFe protein (relative to FeMo-co) have Mo–S bond lengths consistent with either bridging sulfide or terminal thiolate. However, the additional Fe atom, which may also be present in these two sample types, is at a distance only consistent with it being held close to the Mo by a sulfido bridge, based on the structures of synthetic compounds.

These interpretations suggest a scheme to explain the reactions responsible for interconverting these three sample types (Figure 6). One possibility for the protein-to-FeMo-co conversion assumes that a cysteinyl thiolate (or sulfide) S from the protein is bound to a remote site on FeMo-co. The breaking of this FeMo-co–S bond during extraction causes the flexible portion of FeMo-co to "unwrap" from close to the Mo site, which both increases the accessibility of (or creates new) binding sites for ligands and also causes an Fe and a S atom to move away from the Mo. This effect could be initiated by protonation of the protein thiolate (or sulfide). Proton addition is an integral step in the separation of FeMo-co from the protein[9,10] and, perhaps significantly, protons are involved in all substrate reductions.

The suggestion for the FeMo-co to thiolated FeMo-co rearrangement uses the fact that only one added thiolate per FeMo-co[19] causes isolated FeMo-co to assume a structure more closely resembling that within the protein, possibly as shown in Figure 6. The added PhSH/PhSeH might displace the Fe–$S^-$ group from the remote site on FeMo-co, which subsequently binds to the Mo, i.e., it mimics the effect of Cys-$S^-$. The change in the number of atoms in the Fe shell around Mo, which is accommodated by these schemes, is interesting in light of the many proposals made over the years that the end-on $N_2$-binding sites may involve more atoms than the single Mo. If $N_2$ binding involves a linear, end-on Mo–$N_2$–Fe bridge, the distance of 2.7 Å, which we observe, must increase on reduction of the MoFe protein to its $N_2$-binding state in order to accomodate the $N_2$ molecule. In contrast, if $N_2$ binds end-on to one metal (or end-on to one and side-on to the second metal[39]), a smaller accomodation in this distance would suffice.

It may also be relevant to recall that aconitase and certain other Fe–S proteins exhibit variability in their core structures.[40] It is possible that a $MoFe_3S_x \rightarrow MoFe_4S_x$ reaction in nitrogenase could parallel the interconversion of the three-Fe and four-Fe atom clusters in those proteins.

The information on the MoFe protein and its FeMo-co from combined edge and EXAFS studies has thus furthered our understanding of the structure at the Mo site. Studies on substrate- and inhibitor-reacted intermediates will begin to probe how the Mo atom functions in the catalytic cycle. Direct studies of the S atoms in FeMo-co are also now becoming feasible and will allow monitoring of the electronic structure as a function of oxidation state.[41] A single-crystal structure will be ultimately required to fully elucidate the nature of the full Mo–Fe–S site in nitrogenase.

**Acknowledgment.** We gratefully acknowledge the invaluable experimental assistance rendered by Drs. R. A. Scott and J. E. Penner-Hahn. This research was supported by NSF Grant CHE 85-12129 at Stanford University, NSF Grant PCM 81-10335 and NIH Grant R01-AM-30812 at Battelle—Kettering Laboratory, NIH Grant AI 04865-19 at Purdue University, and NIH Grant R01-AM-37255 at the University of California at Davis. The work reported herein was done at Stanford Synchrotron Radiation Laboratory, which is supported by the Department of Energy, Office of Basic Energy Sciences, and the National Institutes of Health, Biotechnology Resource Program, Division of Research Resources.

**Registry No.** Mo, 7439-98-7; nitrogenase FeMo cofactor, 72994-52-6; nitrogenase, 9013-04-1.

**Supplementary Material Available:** Lists of energy versus absorbance for the data sets used in this analysis (27 pages). Ordering information is given on any current masthead page.

(39) Newton, W. E.; Corbin, J. L.; McDonald, J. W. In *Nitrogen Fixation*; Newton, W. E., Nyman, C. J., Eds.; Washington State University: Pullman, WA, 1976; p 53.

(40) Beinert, H.; Emptage, M. H.; Dreyer, J.-L.; Scott, R. A.; Hahn, J. E.; Hodgson, K. O.; Thompson, A. J. *Proc. Natl. Acad. Sci. U.S.A.* **1983**, *80*, 393.

(41) Hedman, B.; Frank, P.; Gheller, S. F.; Roe, A. L.; Newton, W. E.; Hodgson, K. O. *J. Am. Chem. Soc.*, in press.